Metal and dielectric nanoparticle scattering for improved optical absorption in photovoltaic devices

P. Matheu,[a] S. H. Lim, D. Derkacs, C. McPheeters, and E. T. Yu[b]
Department of Electrical and Computer Engineering, University of California, San Diego La Jolla, California 92093-0407, USA

(Received 2 May 2008; accepted 23 June 2008; published online 18 September 2008)

The influence of electromagnetic scattering by Au and silica nanoparticles placed atop silicon photovoltaic devices on absorption and photocurrent generation has been investigated. The nanoparticles produce substantial increases in power transmission into the semiconductor and consequently photocurrent response from ~ 500 to > 1000 nm. Increases in power conversion efficiency under simulated solar irradiation of up to 8.8% are observed experimentally, and numerical simulations provide quantitatively accurate predictions of these observed enhancements. Additional simulations indicate that these concepts can be applied to a broad range of photovoltaic device structures, including those based on low-index materials for which conventional antireflection coatings are problematic. © *2008 American Institute of Physics*.
[DOI: 10.1063/1.2957980]

Commercially available crystalline Si solar cells, which currently dominate the photovoltaics market, typically possess power conversion efficiencies (η) in the range of 10–20%.[1,2] As potential routes to improving η in photovoltaic devices generally, and hence the economic viability of solar power systems, there is extensive interest in light trapping and manipulation techniques including antireflection coatings (ARCs), surface texturing, increasing the optical path length for thin photovoltaic films,[1,2] and optical absorption enhancement via scattering from metallic or dielectric nanoparticles.[3–8] With respect to structures incorporating metal nanoparticles, several references have demonstrated measurable photocurrent enhancement for silicon-on-insulator photodiode structures,[3,4] hydrogenated amorphous Si thin film cells,[5] and crystalline Si *p-n* photodiodes.[6–8] It has been noted that a distinct advantage of nanoparticle scattering is that there is little to no detrimental effect on the electrical properties at the semiconductor surface.[3,4]

In this letter we demonstrate and analyze enhancement of optical absorption in the active semiconductor region of crystalline Si photovoltaic devices using either metallic or dielectric nanoparticles that scatter incident light in a manner favorable for photocurrent generation. By engineering the size, shape, and concentration of nanoparticles, transmission of light into the semiconductor can be enhanced via scattering that occurs preferentially in the forward direction. Scattering by metallic nanoparticles is strongly influenced by localized surface plasmon resonances,[9] leading to effects that can either increase or suppress optical absorption in the semiconducting substrate.[5–8] Dielectric nanoparticles, however, have no plasmon resonance and exhibit a less pronounced effect over a larger range of wavelengths. Mie scattering theory encompasses both the scattering and plasmonic resonance behavior of such particles and provides an accurate basis to help predict the enhancement in η via light scattering.[9] Numerical simulations combined with experimental measurements for commercial grade crystalline Si solar cell devices are employed to demonstrate substantial enhancements in both photocurrent response and photovoltaic power conversion efficiency, elucidate the origins of the observed behavior, and assess merits of silica and metal nanoparticle-based scattering in general as a means of performance improvement in photovoltaics.

The device structures in our experiments consisted of commercially available n^+/p crystalline Si solar cells with front side surface texturing obtained from Silicon Solar, Inc. The pre-existing ARC and metal contacts were chemically stripped using first HF and then $HCl:HNO_3$. New contacts were fabricated using photolithography and lift-off with an active area for each of approximately 1 cm^2. 100 nm diameter Au or 150 nm diameter silica nanoparticles (nanoComposix, Inc.) were deposited on fabricated devices from solutions containing colloidal Au or silica nanoparticles at concentrations between 1×10^{10} and 2×10^{11} ml^{-1}. To improve particle adhesion, samples were first drop coated with poly-l-lysine for 3 min, then rinsed in de-ionized water and blown dry with nitrogen. The colloidal particle solution was also drop coated onto the sample and maintained in a humid environment for 15–120 min, yielding particle concentrations ranging from 4×10^8 to 2×10^9 cm^{-2} with negligible particle clustering. Figure 1 shows both a schematic of the experimental geometry employed and a scanning electron micrograph of Au nanoparticles deposited onto a device from which the particle concentration and absence of clustering can be confirmed.

To measure the photocurrent response, samples were illuminated at normal incidence using a 100 W tungsten-halogen lamp and a 1200 groove/mm grating monochromator, providing monochromatic light at wavelengths of 500–1100 nm. For measurements at wavelengths of 600 nm and longer, a red filter was employed to eliminate illumination from the second-order diffraction line. For each measurement, the illumination spectrum was obtained using a 50/50 beam splitter to direct light to a reference Si photodiode. Current-voltage (*I-V*) characteristics were obtained, either in the dark or under illumination from a 150 W Newport Solar Simulator with a global AM 1.5 direct filter, using a room-temperature probe station and HP 4156A Semiconduc-

[a]Present address: University of California, Berkeley, California 94720, USA.
[b]Electronic mail: ety@ece.ucsd.edu.

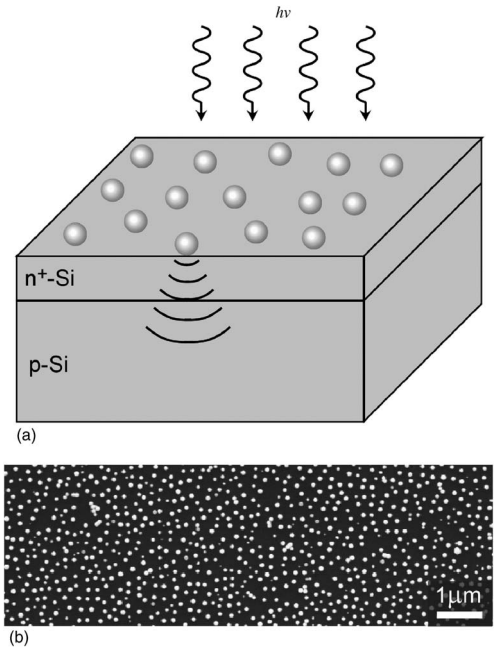

FIG. 1. (a) Schematic of device and experimental geometry, with schematic representation of forward scattered wave. (b) Scanning electron micrograph showing Au nanoparticles deposited on device surface at a concentration of 1.4×10^9 cm^{-2} with minimal particle clustering.

tor Parameter Analyzer. *I-V* measurements of enhanced photocurrent for devices fabricated in the same manner were reproducible to within ~1%.

Numerical simulations using the COMSOL™ finite element simulation software package with the electromagnetics module were employed to optimize nanoparticle concentration and diameter. For silica nanoparticles, the concentration was optimized specifically for a particle diameter of 150 nm. The simulated structures, modeled after experimental devices, consisted of a Au or silica nanoparticle on the surface of an infinitely thick crystalline Si substrate, using established values[10] for the wavelength dependent optical properties of Au, Si, and silica. Different concentrations of nanoparticles were represented by varying the simulation volume and by employing mirror boundary conditions corresponding to a periodic square array of particles on the semiconductor substrate surface.[7]

Figure 2 shows measured *I-V* characteristics under AM 1.5 spectrally filtered illumination for devices with either Au or silica nanoparticles at concentrations of 9.9×10^8 and 1.9×10^9 cm^{-2}, respectively. Clear increases in I_{sc} are observed in the presence of nanoparticles—with the increases ranging from approximately 1% to almost 3% for Au nanoparticle concentrations between 4×10^8 and 2×10^9 cm^{-2}, and from 4% to almost 9% for silica nanoparticle concentrations between 1×10^9 and 3×10^9 cm^{-2}. An increase in the short circuit current leads directly to an increase in the power conversion efficiency $\eta=FFI_{sc}V_{oc}/P_{in}$, where FF, I_{sc}, V_{oc}, and P_{in} are the fill factor, short circuit current, open circuit voltage, and input power, respectively. Small, mostly offsetting, changes in the fill factor and maximum power were observed in the measurements from sample to sample, most likely due to the nonideal nature of the commercial grade cells. The measured change in V_{oc} was less than 0.01 V for all reported samples. Overall, these minimal variations in V_{oc} suggest that the placement of these concentrations of nanoparticles on the photovoltaic device surface influences predominantly I_{sc} and that $\Delta\eta$ is directly proportional to ΔI_{sc}.

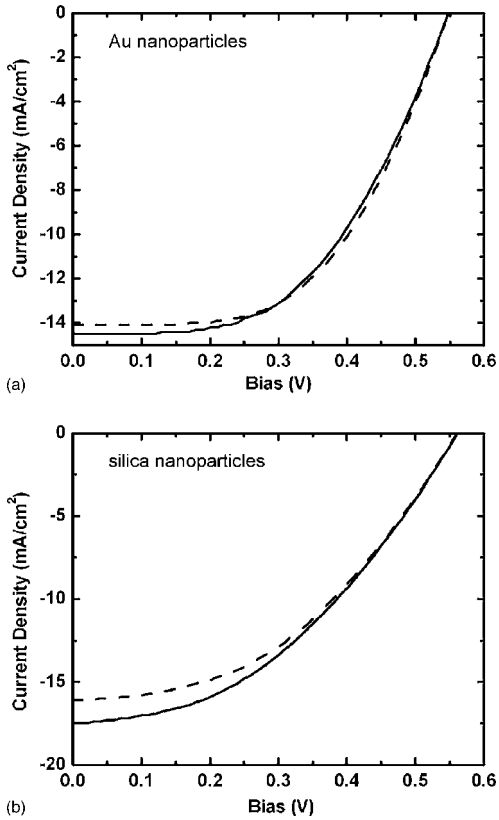

FIG. 2. *I-V* characteristics, under AM 1.5 filtered illumination, for crystalline Si photovoltaic devices, before (dashed) and after (solid) deposition of (a) Au nanoparticles at a density of 9.9×10^8 cm^{-2}, or (b) silica nanoparticles at a density of 1.9×10^9 cm^{-2}. Enhancements in short circuit current densities of 2.8% and 8.8% are observed for Au and silica nanoparticles, respectively.

Figure 3(a) shows experimentally observed ratios of measured photocurrent response spectra for devices on

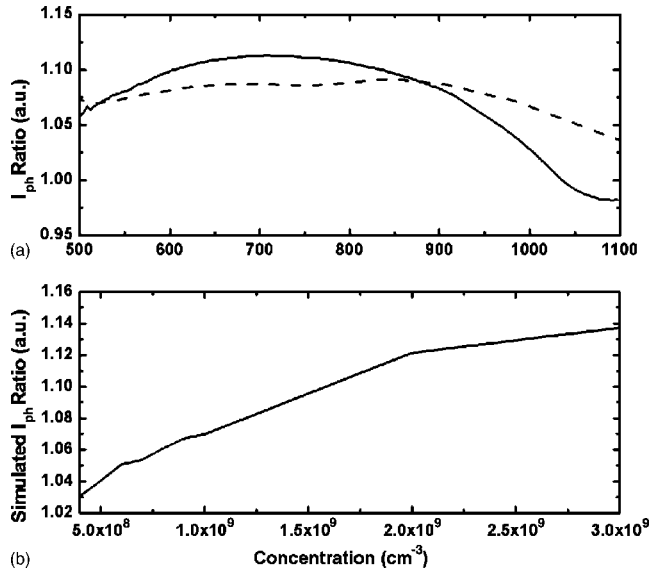

FIG. 3. (a) Measured photocurrent response as functions of wavelength for two devices with silica nanoparticles at concentrations of 1.03×10^9 cm^{-2} (dashed) and 1.92×10^9 cm^{-2} (solid), shown as ratios relative to reference response of the same devices prior to nanoparticle deposition. (b) Numerically simulated enhancement ratio of the projected short circuit current as a function of 150 nm silica nanoparticle concentration.

which silica nanoparticles have been deposited, relative to those of the same devices prior to nanoparticle deposition. For Au nanoparticles, the observed photocurrent response behavior has been analyzed in detail previously[7] in terms of Mie scattering and the phase relationship between the wave scattered by the nanoparticle and that transmitted directly across the air-semiconductor interface. Specifically, the forward scattered light is dominated by a dipolar mode and there can exist, in Mie scattering, a phase mismatch between the dipolar scattered spherical wave front and the planar incident wave front. The phase mismatch can vary with wavelength and lead to wavelength regimes with either constructive or destructive interference. For metal nanoparticles, this phase mismatch is amplified near the plasmon resonance and is closely related to the polarizability of the particle, leading to a reduction in photocurrent response at short wavelengths. Dielectric nanoparticles display a much lower phase mismatch across the spectrum of interest, as well as lower losses compared to the absorptive losses for metal nanoparticles near the plasmon resonance wavelength. Because this phase mismatch is very small for silica nanoparticles compared to that for Au nanoparticles, the observation of photocurrent enhancement, with silica nanoparticles, persists across the entire range of wavelengths shown in Fig. 3(a). A higher silica nanoparticle concentration can further increase the enhancement due to the larger number of scattering sites. Figure 3(a) compares the wavelength resolved enhancement for two concentrations of silica nanoparticles, showing a slight trade-off between the peak photocurrent enhancement and the range of wavelengths over which the photocurrent is enhanced. Figure 3(b) shows the projected photocurrent enhancement ratios from numerical simulations for silica nanoparticle concentrations between 4×10^8 and 3×10^9 cm^{-3}.

At wavelengths far from the Au surface plasmon polariton resonance, the phase shifts associated with scattering from both Au and silica nanoparticles are minimal, and scattered irradiances calculated using classical Mie scattering theory are comparable.[9] For example, scattering in the forward direction at an incident wavelength of 700 nm yields a scattered irradiance per unit incident irradiance of 1.5×10^{-6} for a 150 nm diameter silica particle and 3.3×10^{-7} for a 100 nm diameter Au particle. This is reflected in the comparable magnitudes of the enhancement in photocurrent response for Au and silica nanoparticles, at similar concentrations, for wavelengths substantially longer than the Au surface plasmon polariton wavelength.[7] Finally, we note that integration of the numerically simulated enhancement in photocurrent response, weighted by the AM 1.5 solar irradiation spectrum, yields values in reasonable quantitative agreement with those observed experimentally. Specifically, experimentally observed enhancements of I_{sc} peaked at 2.8% using 100 nm diameter Au nanoparticles at 9.9×10^8 cm^{-2} and at 8.8% using 150 nm diameter silica nanoparticles at 1.9×10^9 cm^{-2}. Numerical simulations at these concentrations predict I_{sc} enhancements of 1.1% and 11.6% for 100 nm diameter Au and 150 nm diameter silica nanoparticles, respectively.

These concepts are readily extended beyond Si to other photovoltaic materials. In general, nanoparticles act as a coupling device to scatter incident light both in the forward direction and laterally into thin film optical modes.[11,12] While our demonstrations reported here employ commercially available crystalline Si solar cells, the universal nature of Mie scattering with small particles implies that particles of a wide range of materials can be engineered to increase the optical transmission of light regardless of the underlying absorbing substrate. For Si solar cells, the resulting increase in photocurrent is smaller than that achievable with conventional ARC technologies. However, our numerical simulations indicate that nanoparticle-based scattering for light trapping may be beneficial for lower-index absorbers, such as organic semiconductors, where traditional antireflection technologies are difficult to apply. For example, the projected short circuit current enhancement for silica nanoparticles on an organic semiconductor poly-3-hexylthiophene substrate at concentrations of 4×10^8 and 2×10^9 cm^{-2} are 1.87% and 7.86%, respectively. Furthermore, nonabsorbing particles, such as silica, should scatter light more efficiently within the AM1.5 spectrum both in the forward direction and into lateral waveguide modes in thin film organic photovoltaic cells when compared with most metallic nanoparticles.

In summary, nanoparticle scattering experiments combined with numerical electromagnetic simulations have provided a greater understanding of the versatility and limitations of nanoparticle-based scattering for increasing photovoltaic performance. I_{sc} enhancements up to 2.8% and 8.8% were measured for crystalline Si photovoltaic devices for Au and silica nanoparticle-based scattering, respectively. Numerical simulations are able to predict the degree of enhancement and agree well with experimental results. While optical absorption enhancement via nanoparticle based scattering is probably of limited benefit when compared to currently available ARC technologies for elemental and compound semiconductor substrates with large refractive indexes, nanoparticle-based scattering may prove useful for lower-index organic photovoltaics or other novel thin film absorbers and detectors.

The authors would like to acknowledge Steven Oldenburg and Thomas Darlington of nanoComposix, Inc. for their advice in nanoparticle deposition methods, and Professor J. M. Xu, Brown University, for discussions on scattering with various nanoparticle materials. Part of this work was supported by a grant from the UCSD Von Liebig Center and by AFOSR (FA9550-07-1-0148).

[1] A. Goetzberger, C. Hebling, and H. W. Schock, Mater. Sci. Eng., R. **40**, 1 (2003).
[2] A. Luque and S. Hegedus, *Handbook of Photovoltaic Science and Engineering* (Wiley, Chichester, 2003), pp. 1–43 and 255–306.
[3] H. R. Stuart and D. G. Hall, Appl. Phys. Lett. **73**, 3815 (1998).
[4] S. Pillai, K. R. Catchpole, T. Trupke, and M. A. Green, J. Appl. Phys. **101**, 093105 (2007).
[5] D. Derkacs, S. H. Lim, P. Matheu, W. Mar, and E. T. Yu, Appl. Phys. Lett. **89**, 093103 (2006).
[6] D. M. Schaadt, B. Feng, and E. T. Yu, Appl. Phys. Lett. **86**, 063106 (2005).
[7] S. H. Lim, W. Mar, P. Matheu, D. Derkacs, and E. T. Yu, J. Appl. Phys. **101**, 104309 (2007).
[8] S. P. Sundarajan, N. K. Grady, N. Mirin, and N. J. Halas, Nano Lett. **8**, 624 (2008).
[9] C. F. Bohren and D. R. Huffman, *Absorption and Scattering of Light by Small Particles*, Wiley Professional Paperback ed. (Wiley, New York, 1998), pp. 69–119 and 326–341.
[10] E. D. Palik and G. Ghosh, *Handbook of Optical Constants of Solids* (Academic, Orlando, 1985), Vol. 1, pp. 286–294, 547–569, and 749–763.
[11] H. R. Stuart and D. G. Hall, Phys. Rev. Lett. **80**, 5663 (1998).
[12] B. J. Soller and D. G. Hall, J. Opt. Soc. Am. B **19**, 1195 (2002).